Preparation, Characterization, and Cellular Interactions of Collagen-Immobilized PDMS Surfaces

I. Keranov,[1] T. Vladkova,[1] M. Minchev,[2] A. Kostadinova,[3] G. Altankov[3]

[1]*Department of Polymer Engineering, University of Chemical Technology and Metallurgy (UCTM), 1756 Sofia, Bulgaria*
[2]*Central Laboratory of Photoprocesses, Bulgarian Academy of Sciences, 1113 Sofia, Bulgaria*
[3]*Institute of Biophysics, Bulgarian Academy of Sciences, 1113 Sofia, Bulgaria*

Received 19 September 2007; accepted 8 February 2008
DOI 10.1002/app.28630
Published online 9 July 2008 in Wiley InterScience (www.interscience.wiley.com).

ABSTRACT: Multistep procedure to biofunctionalization of (poly)dimethylsiloxane (PDMS) surfaces is present here, including plasma-based Ar^+ beam treatment; acrylic acid grafting; and flexible PEG spacer coupling prior to the collagen immobilization by peptide synthesis reaction. The success of any step of the surface modification is controlled by XPS analysis, contact angle measurements, SEM, and AFM observations. To evaluate the effect of PEG chain length, three diNH_2PEGs (2000, 6000, and 20,000 D) of relative long polymer chain were employed as a spacer, expecting that a long flexible spacer could provide more conformational freedom for the collagen molecules and fibroblast reorganization to further cellular matrix formation. Human fibroblast cells were used as a model to evaluate the biological response of the collagen-immobilized PDMS surfaces. It is found that the earlier described biofunctionalization is one more road to improvement of the cellular interaction of PDMS, the last one being the best when PEG spacer with moderate chain length, namely of 6000 D, is used. © 2008 Wiley Periodicals, Inc. J Appl Polym Sci 110: 321–330, 2008

Key words: biomaterials; polysiloxanes; surfaces; modification; nanolayers

INTRODUCTION

Biomolecule (peptides, proteins, etc.) immobilization onto the polymer surface is one of the possible ways to improvement of its interaction with cells—the last one of great importance at the cell culture, tissue engineering, and biointegratable biomaterials. Biomolecule immobilization could be achieved by different techniques based on either physical adsorption or covalent bonding. Unfortunately, the direct covalent bonding of biomolecules to the surface of chemically inert polymers like (poly)dimethylsiloxane (PDMS), (poly)tetrafluorethene (PTFE), etc. is difficult. Therefore, preactivation of such materials surface, followed by a multistep procedure, is necessary. For example, plasma treatment of expanded PTFE, offering a way to peptide immobilization is described in the literature.[1] Cold plasma obtained in low-pressure glow discharge has been often used to activate polymer surface, including siloxane membranes,[2–5] for further grafting of suitable monomers like acrylic acid (AA), hydroxyethylmetacrylate, etc. On the other hand, the ion-beam without following grafting[6,7] is another possible way to improve the biocontact properties of poly(hydroxymethylsiloxane), this effect being confirmed also at PDMS.[8,9] We employed plasma-based Ar^+ beam performed in radio frequency (RF) (13.56 MHz) low-pressure (200 mTorr) glow discharge with a serial capacitance for surface modification of PDMS trying to combine some advantages of both: ion-beam and plasma treatment, namely durability of the modifying effect of the ion-beam with the simplicity of the plasma as compared to ion-beam equipment. The presence of a serial capacitance ensures the arise of an ion flow inside the plasma volume directed toward the treated sample, and the varying discharge power ensures varied ion-flow density. The modifying effect of such treatment is described in detail in our former publications.[10,11] It was interesting to understand how the earlier described treatment influences the initiation of following modification procedures. Therefore, we present here a multistep procedure to PDMS surface biofunctionalization induced by plasma-based Ar^+ beam treatment followed by AA grafting and diNH_2-PEG spacer bonding prior to immobilization of collagen, type I (by peptide synthesis reaction). The success of any step of the surface modification is controlled by XPS analysis, contact angle measurements, SEM, and atom force microscopy observations.

To evaluate the effect of the spacer chain length, we employed three diNH_2-PEGs of different and

Correspondence to: T. Vladkova (TGV@uctm.edu).
Contract grant sponsor: National Fund ''Scientific Investigations,'' Ministry of Education and Science, Bulgaria; contract grant number: NT 2-04/2004.

relative long polymer chain (2000, 6000, and 20,000 D), expecting that the long flexible spacer could provide more conformational freedom for the collagen molecules and the fibroblasts reorganization to cellular matrix formation.

Human fibroblast cells were used as a model to evaluate the biological response of the collagen-immobilized PDMS surfaces.

EXPERIMENTAL

Samples preparation

PDMS thin films (thickness of 50–70 μm) were deposited on prelyophilized cover glasses (15 mm × 15 mm) by spinning of Silopren LSR 2070 (FDA, GE Bayer Silicones, Germany) precursor polymer solution in toluene (5% v/v) and cured in conventional way, as it is described in our former articles.[10,11]

Plasma-based Ar^+ beam treatment

The plasma-based Ar^+ beam treatment of the samples was performed in RF (13.56 MHz) low-pressure (200 mTorr) glow discharge at 1200 W (surface density of the discharge power of 1.1 W/cm^2) for 1 min, the procedure described in detail in Ref. 10.

AA grafting

AA grafting was performed as it is earlier described[10]on plasma-based Ar^+ beam-treated samples kept for 10 min in air and after immersion in water solution (50% v/v) of AA (Merck) at 60°C for 12 h. The grafted samples were taken out of the flasks and washed by Soxhlet extraction with ethanol for 24 h and then rinsed three times with deionized water to remove any adsorbed homopolymers. The amount of surface —COOH groups on the AA-grafted PDMS is 6.3 nmol/m^2.[10]

diNH_2-PEG coupling

AA-grafted PDMS surfaces were reacted with PEG bearing two terminal NH_2 groups, irrespective of diNH_2-PEG_{2000}, diNH_2-PEG_{6000}, or diNH_2-PEG_{20000} in a known way[1]: the AA-grafted PDMS wafers were placed in a flask with 10 mL commercial buffer solution (pH 5) containing 140 mg of (N-(3-dimethylaminopropyl)-N′-ethylvarbodiimide), and the closed flask was kept for 1 h at 4°C for activation of the carboxylic group. Then 40 mL of 0.1 m*M* diNH_2-PEG solution (pH 5) was added, and the reaction was performed for 24 h at 4°C under gentle stirring. At the end of the reaction, the diNH_2-PEG-coupled samples were washed three times with distilled water.

Collagen immobilization

A known peptide synthesis reaction[1,12,13] was used for the immobilization of collagen, type I on the AA-grafted and PEG spacer-coupled PDMS samples. The last ones were placed in a flask with 10 mL commercial buffer solution (pH 5) containing 1 mL collagen type I (Sigma Chemicals Co., St. Louis, MO) (2 mg collagen in 1 mL acetic acid). Then 140 mg of EDC was added, and the immobilization reaction was carried out at 4°C under mild stirring for 24 h. The collagen-immobilized samples were washed three times with distilled water.

XPS analysis

XPS analysis was carried out with ESCALAB II MK VG Scientific spectrometer. The excitation X-ray source was Al Kα (excitation energy: 1486.6 eV). Complete spectral scans as well as detailed recordings of the main peaks were made at 10^{-8} Pa. The binding energy scale was fixed by assigning E_b = 285 eV to C1: C—C or CH C1s peak. According to previous studies[1,10,11,14] and using this reference peak, the carbon chemical shifts for different oxygen containing groups are

C2: from hydroxyl, hydroperoxide, ether, alkyl, or sulfate ester, ΔE_b = 1.5 eV;
C3: >C=O from carbonyl or amide, ΔE_b = 3.0 eV;
C4: —COO— from carboxyl or the corresponding ester, ΔE_b = 4.2 eV.

The different peak area was computed graphically and corrected by using Scofields relative cross sections.[14]

Contact angle measurements

Modified method of Bikerman[15,16] was used to evaluate the equilibrium contact angle of two liquids with known surface tension: polar H_2O (γ_{lv} = 72.8 mJ/m^2, γ^d_{lv} = 21.8 mJ/m^2, and γ^p_{lv} = 51.0 mJ/m^2) and nonpolar CH_2J_2 (γ_{lv} = 50.8 mJ/m^2, γ^d_{lv} = 49.5 mJ/m^2, and γ^p_{lv} = 1.3 mJ/m^2) measuring the diameter of three drops of each volume: 1 μL, 2 μL, 3 μL. Surface tension and its polar and disperse components as well as the polarity of the modified surfaces were calculated according to Kaelble's equation.[17,18]

SEM observation

The surface morphology of PEG-coupled and collagen-immobilized PDMS surfaces was observed by SEM, Philips-515.

AFM

AFM in tapping mode (AFM device: Nanoscope-3, Digital instruments, Santa Barbara, CA) using a

single crystal silicone probe (model TESP) with a spring constant of 0.58 N/m was employed to obtain more detailed information about the surface topography and roughness. The scanning frequency was 1 Hz.

Mean roughness, R_a (in nm), was calculated using the following equation:

$$R_a = \frac{1}{L_x L_y} \int_0^{L_y} \int_0^{L_x} [f(x,y)]\, dx\, dy$$

where L_x and L_y are dimensions of the surface.

Root mean square, R_q (in nm), was calculated as standard deviation of the Z values within the given area as shown:

$$R_q = \sqrt{\frac{\sum (Z_i - Z_{ave})^2}{N}}$$

where Z_{ave} is the average of the Z values within the given area Z_i; Z_i, current Z value; N, number of points within given area.

Cells

Human fibroblasts were prepared from fresh skin biopsy and used up to the ninth passage. The cells were grown in Dulbecco's minimal essential medium (DMEM) containing 10% fetal bovine serum (Sigma) in a humidified incubator with 5% CO_2. For the experiments, the cells were harvested from nearly confluent cultures with 0.05% trypsin/0.6 m*M* EDTA (Sigma).

Initial cellular interaction

The initial cellular interaction was characterized by monitoring the overall cell morphology of fibroblasts adhering for 2 h on aforementioned surfaces precoated with FN. Briefly, 15 mm × 15 mm samples prepared as mentioned earlier and were placed in six-well TC plates (Costar) and washed 3× with PBS. All samples were precoated with FN (see later). 3×10^5 cells per well was added and incubated for 2 h in humidified CO_2 incubator at 37°. Than the samples were viewed at 20× magnifications on the inverted phase contrast microscope (type Fluoval 20, Zeiss, Germany) equipped with a digital camera.

Overall cell morphology

Approximately 5×10^5 cells per well were incubated in serum-free medium (DMEM) for the times indicated in six-well polystyrene plates (Falcon Becton Dickinson) containing PDMS samples. Half of them were precoated with 20 mg/mL FN (30 min in PBS). At the end of the incubation, the samples were studied and photographed in an inverted phase contrast microscope (Axiovert, Zeiss, Germany).

Immunofluorescence for fibronectine (FN) matrix

To study FN matrix formation, human fibroblasts were cultured for 3 days in six-well TC plates containing the samples at initial seeding density of 1×10^5 cells per well. Than samples were washed with PBS, fixed for 5 min with 3% paraformaldehyde (in PBS), and saturated for 15 min with 1% bovine serum albumin (BSA; Sigma). To visualize FN, the samples were incubated for 30 min at room temperature with anti-FN monoclonal antibody (Sigma Cat. No F 7387) diluted 1 : 100 in 1% BSA in PBS followed by Cy2-conjugated goat anti-mouse secondary antibody (Dianova Germany) 1 : 100 in 1% goat serum in PBS. Finally, the samples were washed 3× in PBS, mounted in Moviol, and viewed on the fluorescence microscope (Fluoval 20) using the green (fluorescin isothio cianat) channel. The images were captured with a CCD camera.

RESULTS AND DISCUSSION

Surface chemical composition, wettability, topography, and roughness were controlled on every stage of the multistep collagen immobilization procedure, namely of (1) plasma-based Ar^+ beam treated; (2) AA-grafted; (3) PEG-coupled; and (4) collagen-immobilized surface. All surface characteristics of both plasma-based Ar^+ beam-treated and AA-grafted surfaces are discussed in detail earlier.[2,3] We present here experimental results, mainly for PEG-coupled and collagen-immobilized PDMS surfaces. Some surface characteristics of the starting nonmodified as well as of plasma-based Ar^+ beam treated and AA-grafted PDMS are included for comparison.

The main alteration of the surface chemical composition due to the plasma-based Ar^+ beam treatment occurs in the first minute at 1200 W, as we found in previous investigation.[10] Therefore, the samples for the further AA grafting were treated under these conditions (1200 W/1 min). Twelve-hour AA-grafted samples were employed for the further PEG coupling and collagen immobilization because of their densest grafting. Expecting that the relatively long flexible spacer would provide more conformational freedom of the immobilized collagen molecules, and hence, the fibroblast cells reorganize to form a cellular matrix; three diNH_2-PEGs (2000, 6000, and 20,000 D) of relative long polymer chain were employed to evaluate the spacer chain length effect on the cell response.

TABLE I
Atomic Composition of Varied PDMS Samples Derived from XPS Analysis

	Sample	C (at %)	O (at %)	Si (at %)	N (at %)	S (at %)	Si/C	Si/O
1	PDMS nonmodified	49.7	24.4	25.8	–	–	0.5	1.1
2	PDMS plasma-based Ar^+ beam treated	18.6	49.4	31.0	–	–	1.7	0.6
3	PDMS plasma-based Ar^+ beam treated and AA-grafted	32.8	39.3	28.0	–	–	0.8	0.7
4	PDMS plasma-based Ar^+ beam treated, AA-grafted and di-NH_2-PEG_{2000} coupled	51.0	28.3	17.1	3.6	–	0.3	0.6
5	PDMS plasma-based Ar^+ beam treated, AA-grafted and di-NH_2-PEG_{6000} coupled	54.2	26.8	14.3	4.4	–	0.3	0.5
6	PDMS plasma-based Ar^+ beam treated, AA-grafted and di-NH_2-PEG_{20000} coupled	49.6	28.8	18.1	3. 5	–	0.4	0.6
7	PDMS plasma-based Ar^+ beam treated, AA-grafted, di-NH_2-PEG_{2000}-coupled and collagen-immobilized	58.5	21.3	8.6	11.2	0.4	0.1	0.4
8	PDMS plasma-based Ar^+ beam treated, AA-grafted, di-NH_2-PEG_{6000}-coupled and collagen-immobilized	57.6	24.1	9.6	8.4	0.3	0.2	0.4
9	PDMS plasma-based Ar^+ beam-treated, AA-grafted, di-NH_2-PEG_{20000}-coupled and collagen-immobilized	48.8	27.3	18.4	5.1	0.4	0.4	0.7

XPS analysis

The results of the XPS analysis are summarized in Table I and Figures 1 and 2. The comparison of the chemical composition of the nonmodified and plasma-based Ar^+ beam treated PDMS (Table I, rows 1 and 2) shows the effective altering of the surface chemical composition of the starting PDMS: the oxygen content rises to 49.4% simultaneously with a significant decrease of the carbon content down to 18.6%, and both Si/C and Si/O ratios alter significantly after the treatment, the reason being explained in detail in our former publication.[10] The AA grafting changes additionally the surface chemical composition of the plasma-treated PDMS (Table I, compare rows 2 and 3): silica content decreases down to 28% and both Si/C and Si/O ratios alter again. In the deconvoluted C1s peak [Fig. 1(a)] is observed a new component fitted at 289.2 ± 0.4 eV, indicating the presence of —COO groups on the surface, and these results are discussed in detail earlier.[10,11] The carboxylic groups available on the AA-grafted PDMS surface were used for coupling of diNH_2-PEG to play a flexible anchor between the surface and the collagen. The covalent attachment of diNH_2-PEG to the surface is confirmed by the detection of significant amount (3.5–4.4 at %) of nitrogen on the diNH_2-PEG-coupled surface (Table I, rows 4–6). In addition, as it is evident from Figure 1, the component of ether carbon in the C1s peak centered at 286.5 ± 0.4 eV significantly increases for the PEG-coupled surfaces [compare Fig. 1(b–d) to Fig. 1(a)]. A comparison of the ether component of the carbon peak (at 286.5 ± 0.4 eV) in Figure 1(b–d) shows some differences in their intensity. The calculated ether C1s peck component (at 286.5 ± 0.4 eV) area is of 2.85%, 2.84%, and 3.26% for the PEG_{2000}, PEG_{6000}, and PEG_{20000} bonded surfaces, irrespectively, and this result demonstrates that the ethylene oxide chain density on PEG_{20000} bonded surface is higher as compared to that of the other. The detailed N1s spectra, represented in Figure 2(a–c), exhibit two components centered at about 400.5 ± 0.4 and 402.9 ± 0.4 eV, which are thought to derive respectively from amine and amide groups on the surface, i.e., nonreacted terminal amino groups of the diNH_2-PEG and amide-bonded nitrogen as a result of interaction between

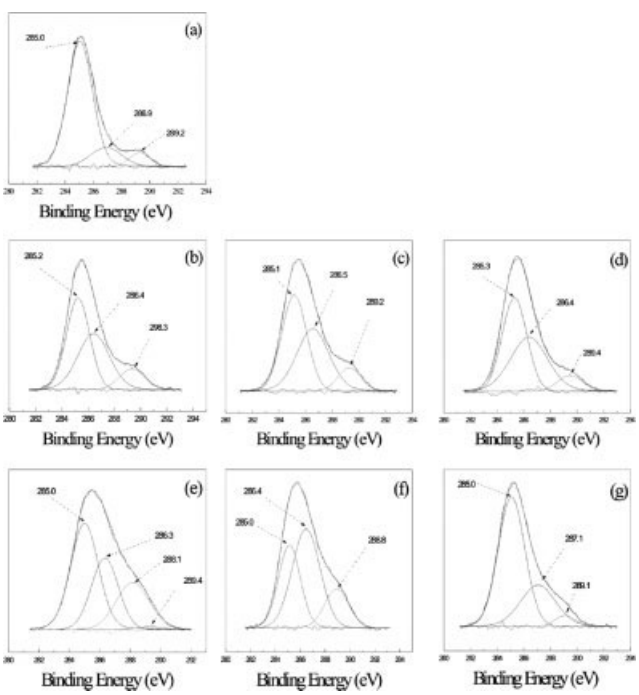

Figure 1 C1s photoelectron peaks and fitted curves of preliminary plasma-activated PDMS: (a) AA-grafted; (b) AA-grafted/diNH_2-PEG_{2000}-coupled; (c) AA-grafted/diNH_2-PEG_{6000}-coupled; (d) AA-grafted/diNH_2-PEG_{20000}-coupled; (e) AA-grafted/diNH_2-PEG_{2000}-coupled/collagen-immobilized; (f) AA-grafted/diNH_2-PEG_{6000}-coupled/collagen-immobilized and (g) AA-grafted/diNH_2-PEG_{20000}/collagen-immobilized.

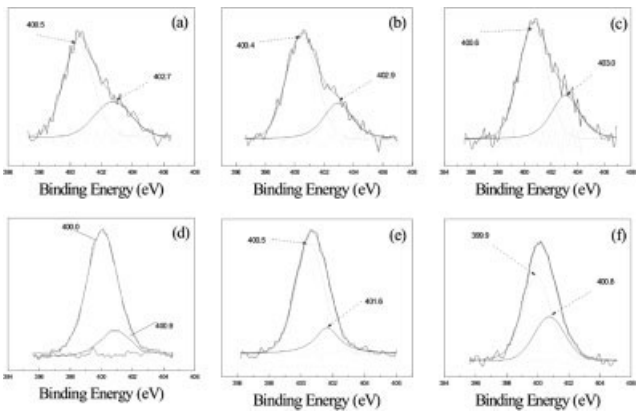

Figure 2 N1s photoelectron peaks and fitted curves of preliminary plasma activated PDMS: (a) AA-grafted; (b) AA-grafted/diNH_2-PEG_{2000}-coupled; (c) AA-grafted/diNH_2-PEG_{6000}-coupled; (d) AA-grafted/diNH_2-PEG_{20000}-coupled; (e) AA-grafted/diNH_2-PEG_{2000}-coupled/collagen-immobilized; (f) AA-grafted/diNH_2-PEG_{6000}-coupled/collagen-immobilized; and (g) AA-grafted/diNH_2-PEG_{20000}/collagen-immobilized.

NH_2-groups of the PEG-spacer and —COOH of the AA-grafted surface. As it is evident form Table I, the nitrogen content is highest (4.4 at %) on the PEG_{6000} bonded surface (compare rows 4–6). The calculated area of the N1s peak component at 400.5 ± 0.4 eV (—NH_2) is of 68.9%, 70.6%, and 67.8% for the PEG_{2000}, PEG_{6000}, and PEG_{20000} bonded surfaces, respectively, i.e., the highest value is again for the PEG_{6000} bonded surface. The highest nitrogen content on the PEG_{6000} bonded surface in a combination with the largest peak area of the NH_2 component of the N1s peak for the same surface indicates that the —NH_2 groups density on it is the highest.

Evidence for the successful immobilization of collagen comes from the presence of low amount of sulfur, as reviled by XPS (Table I, rows 4–6). This outcome could only be explained with the presence of the sulfur-containing amino acids in the collagen, methionine, and cysteine.[19,20] A comparison of the corresponding nitrogen N1s peaks before [Fig. 2(a–c)] and after collagen immobilization [Fig. 2(d–f)] demonstrates significant altering of their profile, confirming in this way the effective immobilization of the collagen. No further information can be derived from the C1s [Fig. 1(e–g)] or N1s [Fig. 2(d–f)] signals because of the complexity of the surface chemistry after the collagen immobilization. At this stage of the experimentation, it is not possible to infer about any intermolecular reaction accruing among the collagen molecules in solution.

Si is detected at every stage of the PDMS surface modification (Table I) indicating that Si2p peak is not fully hidden even at the last stage of the modification, i.e., not enough dense and tick modified layer is formed to fully cover the surface of the starting PDMS.

Contact angles, polarity, surface tension, and its components

The XPS data were to a certain extent validated by the contact angle measurements (Table II). The water contact angle (WCA) of the very hydrophobic PDMS of 101.9° significantly decreases at every stage of the modification, and the surface becomes more or less wettable depending on the nature of the corresponding treatment or coating (Table II, compare row 1 to rows 2–9). In addition, the surface tension, γ_s and polarity, p of the nonmodified PDMS increase mainly due to the increase of the polar component of the surface tension, γ_s^p, depending on the same factors.

Surface morphology and roughness

SEM images of the nonmodified PDMS surface as well as of the modified surfaces on every step of the

TABLE II
Static Contact Angle (θ), Surface Energy (γ), and Polarity (*p*) of Nontreated and Surface-Modified PDMS Samples

	Sample	θ_{H_2O}(°)	$\theta_{CH_2J_2}$(°)	γ_s (mJ/m^2)	γ_s^d (mJ/m^2)	γ_s^p (mJ/m^2)	Polarity (p)
1	PDMS nonmodified	101.9	70.2	22. 9	21.8	1.1	0.05
2	PDMS plasma-based Ar^+ beam treated	60.8	49.5	45.6	28.1	17.5	0.38
3	PDMS plasma-based Ar^+ beam treated and AA-grafted	73	55	36.9	26.6	10.3	0.28
4	PDMS plasma-based Ar^+ beam treated, AA-grafted and di-NH_2-PEG_{2000} coupled	20.1	43.2	69.04	26.94	42.10	0.61
5	PDMS plasma-based Ar^+ beam treated, AA-grafted and di-NH_2-PEG_{6000} coupled	15.9	54.8	70.03	20.73	49.29	0.70
6	PDMS plasma-based Ar^+ beam treated, AA-grafted and di-NH_2-PEG_{20000} coupled	10.6	64.5	72.24	15.56	56.68	0.78
7	PDMS plasma-based Ar^+ beam treated, AA-grafted, di-NH_2-PEG_{2000}-coupled and collagen immobilized	40.0	51.0	57.75	24.48	33.28	0.58
8	PDMS plasma-based Ar^+ beam treated, AA-grafted, di-NH_2-PEG_{6000}-coupled and collagen-immobilized	46.7	78.1	52.42	10.51	41.64	0.74
9	PDMS plasma-based Ar^+ beam treated, AA-grafted, di-NH_2-PEG_{20000}-coupled and collagen-immobilized	47.5	66.6	51.18	16.74	34.44	0.67

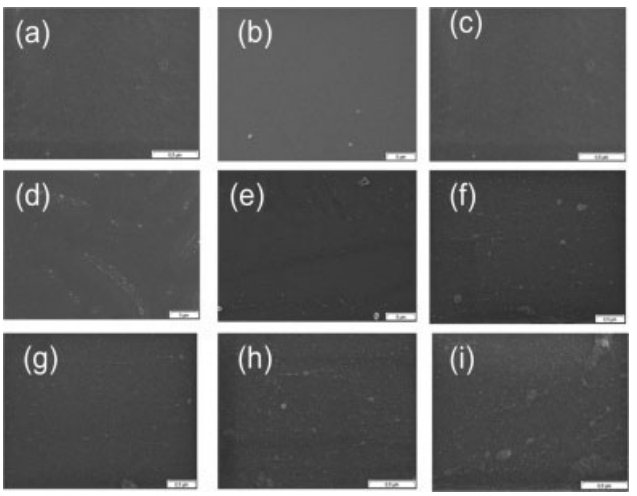

Figure 3 SEM images of (a) nonmodified PDMS; (b) plasma-based Ar^+ beam treated at 1200 W/1 min; (c) AA-grafted for 12 h; (d) $diNH_2$-PEG_{2000}-coupled; (e) $diNH_2$-PEG_{6000}-coupled; (f) $diNH_2$-PEG_{20000}-coupled; (g) $diNH_2$-PEG_{2000}-coupled/collagen-immobilized; (h) $diNH_2$-PEG_{6000}-coupled/collagen-immobilized; and (i) $diNH_2$-PEG_{20000}-coupled/collagen-immobilized.

modification are shown in Figure 3(a–i). The nontreated PDMS [Fig. 3(a)] and all modified surfaces seem to be very smooth [Fig. 3(b–i)], but PEG-coupled [Fig. 3(d–f)] and collagen-immobilized [Fig. 3(g–i)] surfaces demonstrate specific morphology that is thought to be due to the appearance of new phases, PEG or PEG and collagen on the surface, as it was proven by the XPS analysis (Table I, Figs. 1 and 2).

AFM study was performed to obtain more in detail information about the surface morphology and roughness.

The surface of the nonmodified PDMS is relatively smooth: R_a = 1.59 nm and R_q = 2.01 nm (Table III, row 1) and demonstrates small-grain surface topography (Fig. 4), similar to that observed by other authors'.[21] As it is evident from Figure 5, the surface topography retains similarity after the plasma-based Ar^+ beam treatment. But the surface roughness, both R_a and R_q, decreases down to 1.20 and 1.06, respectively, (Table III, row 2). The comparison of AFM images represented in Figure 6 to this represented in Figure 5 clearly shows that they are quite different: the AA-grafted surface (Fig. 6) characterizes with mainly grain topography and appearance of a small number of peaks. The surface roughness increases sharply after AA grafting. R_a and R_q get to 3.80 and 13.66 nm, irrespectively (Table III, row 3). Evidently, the observed altering of the surface morphology and roughness of the plasma-based Ar^+ beam treated PDMS surface (Fig. 5; Table III, row 2) is due to the presence of grafted AA, proven by XPS; classical chemical analysis and hydrophilic/hydrophobic balance of the surface.[2,3]

The drastic altering of the surface topography (compare Figs. 7–9 to Fig. 6) and the change of the surface roughness (Table III, compare rows 4–6 to row 3) confirm the presence of coupled PEG, proven by earlier described XPS analysis and contact angle measurements.

All 2D images in Figures 7–9 indicate significantly increased surface inhomogenity after PEG coupling. In addition, the 3D images show an increased number of peaks and in fact disappearance of the main grain structure of the AA-grafted surface (compare to Fig. 6). The observed deviations in the surface topography (Figs. 7–9) and roughness (Table III, rows 4–6) of the three PEG-coupled samples are evidently due to the different PEG chain length. As it is evident from Table III, both R_a and R_q depend on the length of the PEG chain. As longer is it as higher are both R_a and R_q.

2D (a–c) and 3D (d) AFM images of the same surfaces after immobilization of collagen, type I (via

TABLE III
Mean Roughness (R_a) and Root Mean Square Roughness (R_q) of Nontreated and Surface-Modified PDMS Samples

	Sample	Scan size (μm)	R_a (nm)	R_q (nm)
1	PDMS non-modified	25	1.59	2.01
2	PDMS plasma-based Ar^+ beam treated	25	1.20	1.06
3	PDMS plasma-based Ar^+ beam treated and AA-grafted	25	3.80	13.66
4	PDMS plasma-based Ar^+ beam treated, AA-grafted and di-NH_2-PEG_{2000} coupled	25	3.77	9.94
5	PDMS plasma-based Ar^+ beam treated, AA-grafted and di-NH_2-PEG_{6000} coupled	25	6.50	12.13
6	PDMS plasma-based Ar^+ beam treated, AA-grafted and di-NH_2-PEG_{20000} coupled	25	13.04	23.99
7	PDMS plasma-based Ar^+ beam treated, AA-grafted, di-NH_2-PEG_{2000}-coupled and collagen immobilized	25	16.52	30.05
8	PDMS plasma-based Ar^+ beam treated, AA-grafted, di-NH_2-PEG_{6000}-coupled and collagen-immobilized	25	7.81	20.45
9	PDMS plasma-based Ar^+ beam treated, AA-grafted, di-NH_2-PEG_{20000}-coupled and collagen- immobilized	25	2.73	4.70

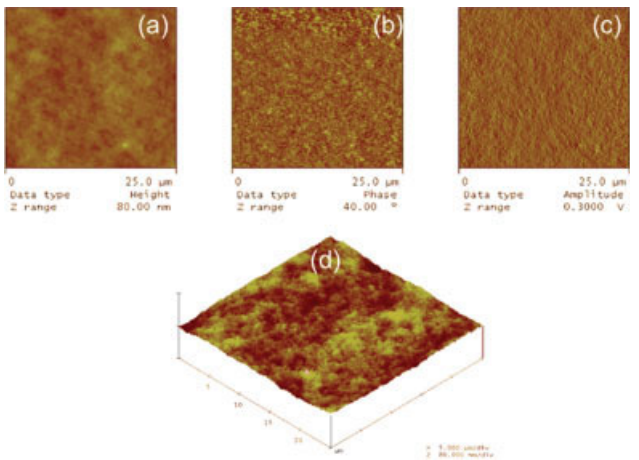

Figure 4 AFM images of nonmodified PDMS surface: (a) 2D height, (b) 2D phase and (c) 2D amplitude; (d) 3D. [Color figure can be viewed in the online issue, which is available at www.interscience.wiley.com.]

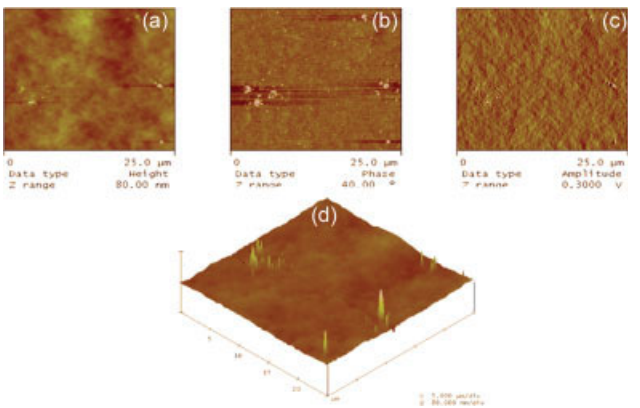

Figure 6 AFM images of plasma-based Ar^+ ion-beam treated and AA-grafted PDMS surface: (a) 2D height, (b) 2D phase, and (c) 2D amplitude; (d) 3D. [Color figure can be viewed in the online issue, which is available at www.interscience.wiley.com.]

PEG spacer of different chain length) are represented in Figures 10–12 and their surface roughness in Table III, rows 7–9, irrespectively. Evidently, the collagen immobilization changes additionally the surface inhomogenity, topography, and roughness (Table III, rows 7–9), and this is thought to be an indirect confirmation for the presence of immobilized collagen on the PDMS surface. The number, height, and shape of the peaks in the 3D images are altered after collagen immobilization [compare 3D images before and after collagen immobilization, irrespectively Figs. 10(d) to 7(d); Figs. 11(d) to 8(d) and Figs. 12(d) to 9(d)]. The most interesting in the 2D images of the same surfaces is the appearance of fibrils in addition to the main surface morphology best expressed when the chain length of the PEG is moderate (PEG_{6000}) [Fig. 11(a–c)]. The length of the PEG chain influences also the surface roughness of the collagen-immobilized surfaces but in manner opposite to the PEG-coupled surface. In this case, as longer is the PEG chain as lower is the surface roughness, and both R_a and R_q decreases sharply with the increase of PEG chain length (Table III, rows 7–9).

Overall cell morphology

The overall cell morphology of fibroblasts adhering for 2 h on PEG_{2000}, PEG_{6000}, and PEG_{20000}-coupled [Fig. 13(a–c)] and collagen-immobilized [Fig. 13(d–f)] PDMS surfaces are represented in Figure 13. It is evident that the fibroblast number on all three PEG-coupled surface is less, compared to that of the corresponding collagen-immobilized one [Fig. 13,

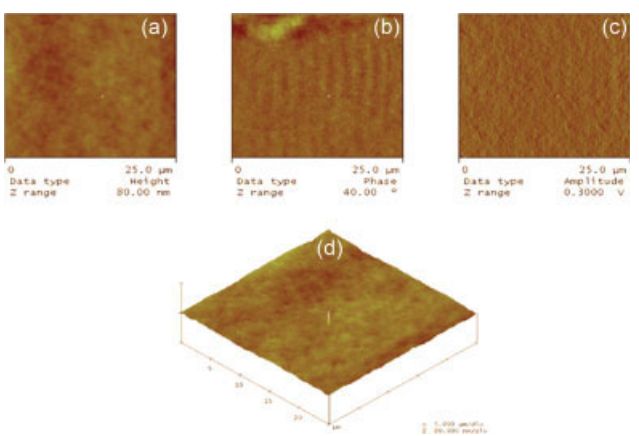

Figure 5 AFM images of plasma-based Ar^+ ion-beam treated PDMS surface performed at constant duration of 1 min at 1200 W: (a) 2D height, (b) 2D phase and (c) 2D amplitude; (d) 3D. [Color figure can be viewed in the online issue, which is available at www.interscience.wiley.com.]

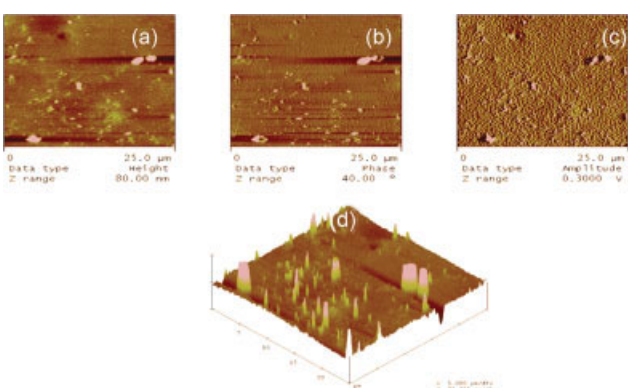

Figure 7 AFM images of plasma-based Ar^+ ion-beam treated, AA-grafted, and diNH_2-PEG_{2000}-coupled PDMS surface: (a) 2D height, (b) 2D phase, and (c) 2D amplitude; (d) 3D. [Color figure can be viewed in the online issue, which is available at www.interscience.wiley.com.]

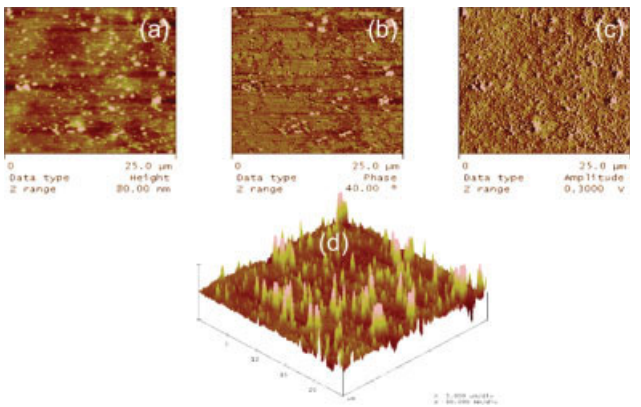

Figure 8 AFM images of plasma-based Ar^+ ion-beam treated, AA-grafted and diNH_2-PEG_{6000} PDMS surface: (a) 2D height, (b) 2D phase, and (c) 2D amplitude; (d) 3D. [Color figure can be viewed in the online issue, which is available at www.interscience.wiley.com.]

compare (a–d), (b–e), and (c–f)]. In addition, the fibroblasts on the PEG-coupled surfaces represent a round shape [Fig. 13(a–c)] because of their disturbed spreading. The last one could be explained by the strong hydrophilic nature of these surfaces characterizing, with a WCA of about 10–20° (Table II, rows 4–6). It is well known[22]that the strong hydrophilic surfaces do not support the initial interaction with living cells. The different fibroblasts number on the three PEG couplet surfaces [Fig. 13(a–c)] could be due to the simultaneous influence of their hydrophilicity (Table II, rows 4–6) and roughness (Table III, rows 4–6), both depending on the PEG chain length.

The cell behavior is quite different after collagen, type I, immobilization on these PEG-coupled surfaces. Evidently, the fibroblast adhesion and spreading are much better on all collagen-immobilized surfaces

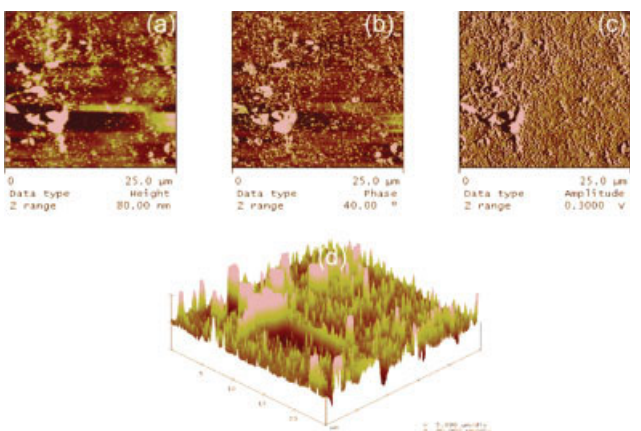

Figure 9 AFM images of plasma-based Ar^+ ion-beam treated, AA-grafted and diNH_2-PEG_{20000} PDMS surface: (a) 2D height, (b) 2D phase, and (c) 2D amplitude; (d) 3D. [Color figure can be viewed in the online issue, which is available at www.interscience.wiley.com.]

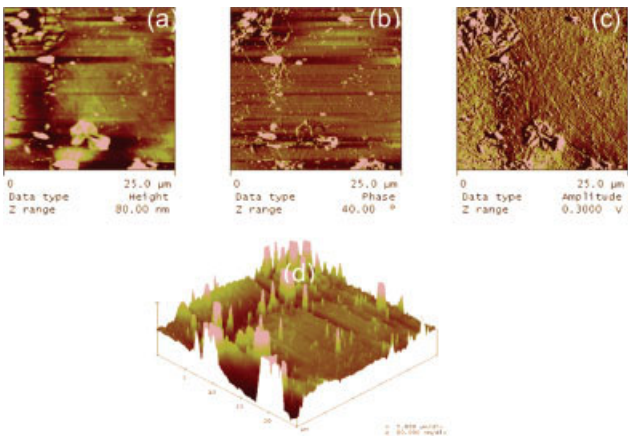

Figure 10 AFM images of plasma-based Ar^+ ion-beam treated, AA-grafted, diNH_2-PEG_{2000}-coupled and collagen-immobilized PDMS surface: (a) 2D height, (b) 2D phase, and (c) 2D amplitude; (d) 3D. [Color figure can be viewed in the online issue, which is available at www.interscience.wiley.com.]

[Fig. 13(d–f)] compared to the corresponding PEG-coupled surfaces [Fig. 13(a–c)], these effects depending on the chain length of the PEG spacer (Fig. 13, compare (d,e, f). As it is evident (Table II, rows 7–9), the PEG chain length influences slightly the surface hydrophilicity of the collagen-immobilized surfaces and the θ_{H_2O} deviations are in the range of 40.0–47.5°, but significantly, and their roughnesses R_a and R_q (Table III, rows 7–9) vary in the range of 16.5–2.7 nm and 30.0–4.7 nm, respectively. The moderate hydrophilicity, accepted now[22]as an important prerequisite for good interactions with living cells, could be a reason for the observed improved cellular interactions of the studied collagen-immobilized PDMS surfaces having θ_{H_2O} = 40.0–47.5°. In addition, we should have for that the collagen immobilization

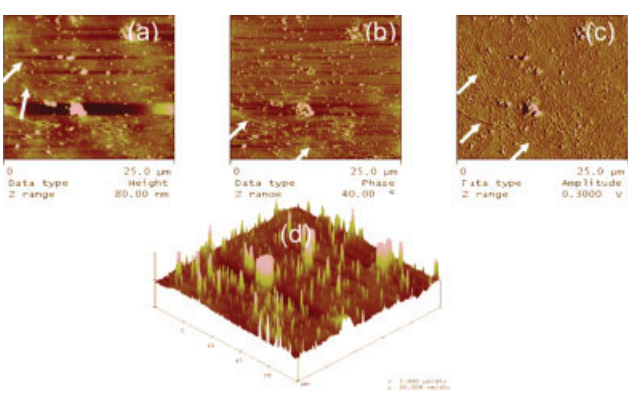

Figure 11 AFM images of plasma-based Ar^+ ion-beam treated, AA-grafted, diNH_2-PEG_{6000}-coupled, collagen-immobilized PDMS surface: (a) 2D height, (b) 2D phase, and (c) 2D amplitude; (d) 3D. [Color figure can be viewed in the online issue, which is available at www.interscience.wiley.com.]

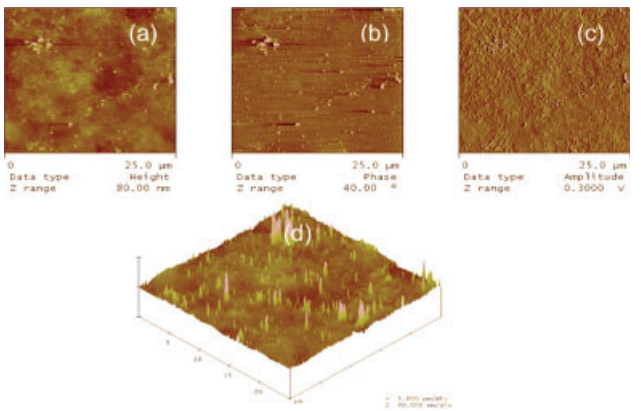

Figure 12 AFM images of plasma-based Ar^+ ion-beam treated, AA-grafted, diNH_2-PEG_{20000}-coupled, collagen-immobilized PDMS surface: (a) 2D height, (b) 2D phase, and (c) 2D amplitude; (d) 3D. [Color figure can be viewed in the online issue, which is available at www.interscience.wiley.com.]

was performed via a PEG spacer. The flexible spacer chain could provide collagen conformations suitable for an easier identification of its RGD sequences and thus for better interactions with the cells. Evidently, an optimal chain length of the PEG spacer exists at with the collagen molecule conformational freedom is optimal for its reorganization and formation of a surface with an optimal roughness and situation of RGD sequences at which the interactions with the

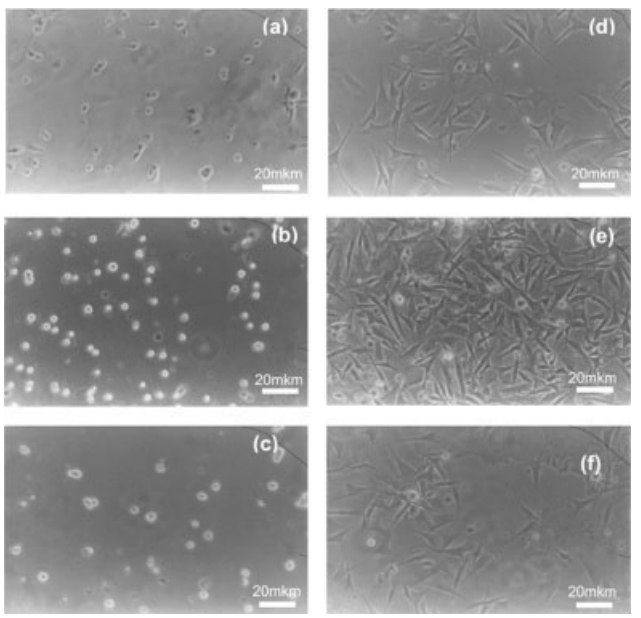

Figure 13 Overall cell morphology of human fibroblast cells on plasma-based Ar^+ ion-beam treated and AA-grafted PDMS surfaces, coupled with PEG-spacer: (a) diNH_2-PEG_{2000}, (b) diNH_2-PEG_{6000}, (c) diNH_2PEG_{20000} and collagen-immobilized: (d) diNH_2-PEG_{2000}-coupled/collagen, (e) diNH_2-PEG_{6000}-coupled/collagen, (f) diNH_2-PEG_{20000}-coupled/collagen.

fibroblast cells are optimal. The largest number of well-speeded fibroblast, i.e., the best initial cellular interaction is observed when the collagen immobilization is performed via diNH_2-PEG_{6000} spacer [Fig. 13(e)], i.e., the optimal PEG chain length in our case is of 6000 D. Another contribution to the best cellular interaction of PEG_{6000} bonded and collagen-immobilized surface could be the expected higher amount of the immobilized collagen on this surface, presumably because of the higher density of surface NH_2 groups (as proven by XPS) acting as bonding points for the collagen —COOH groups. Then the substrate PDMS Si should be better hidden, and Si content on this surface should be the lowest. But if one has a look on Table I, the last three rows 7–9, it gets clear that the surface collagen coating should be of different density, and the last one does not depend on the immobilized collagen amount. Therefore, it could be accepted that the conformational freedom is the predominant factor influencing the cellular interaction.

LDH cell proliferation test

The functional behavior of the fibroblast cells on the PEG-coupled and collagen-immobilized PDMS surfaces was further characterized by measurement of their proliferation. The results are summarized in Figure 14. The cell activity on all studied surfaces increases in the course of cultivation up to 7 days, as it is evident from this figure. The diNH_2-PEG-coupled surfaces (diNH_2-PEG_{2000}, diNH_2-PEG_{6000}, and diNH_2-PEG_{20000}) demonstrate less pronounced cell proliferation as compared to the corresponding collagen-immobilized PDMS surfaces (PEG_{2000} +collagen, PEG_{6000}+collagen and PEG_{20000}+collagen) in correspondence with their too high hydrophilicity

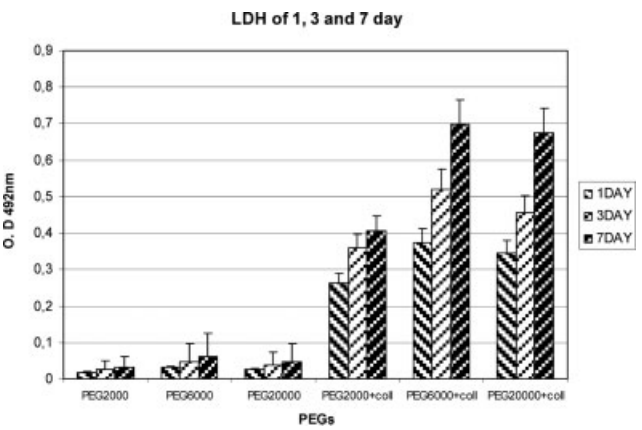

Figure 14 One, 3, and 7 days LDH cell assay on diNH_2-PEG_{2000}-, diNH_2-PEG_{6000}, and diNH_2-PEG_{20000}-coupled or on the same PEG-coated PDMS surfaces after collagen, type I immobilization.

(θ_{H_2O} = 20.1–10.6°). The 1, 3, and 7 days fibroblasts proliferation is the best on $diNH_2$-PEG_{6000}-coupled surface as compared to the $diNH_2$-PEG_{2000} and $diNH_2$-PEG_{20000}-coupled surfaces. Similar result was found earlier for PEI/PEG_{6000}-coated surface.[23]

One, 3, and 7 days LDH assay on collagen-immobilized surfaces confirms the earlier described results of our overall cell morphology observations. The cell activity increases in the course of incubation up to 7 days on all collagen-immobilized surfaces, and the cell proliferation remains the highest when the collagen immobilization is performed via $diNH_2$-PEG_{6000} PDMS surface after 3 and 7 days of incubation. This confirms that the optimal chain length of the PEG spacer is of 6000 D.

CONCLUSIONS

Plasma-based Ar^+ beam treatment initiated multistep procedure is performed to biofunctionalization of strong hydrophobic chemically inert PDMS.

The successful surface modification at every step is confirmed by XPS analysis, contact angle measurements, SEM, and AFM observations.

Collagen immobilization via flexible spacer improves the cellular interactions of the scarcely adhesive PDMS surface significantly, depending on the chain length of the PEG chain.

The moderated PEG chain length (of 6000 D) is preferable because it is optimal for the initial adhesion and proliferation of the fibroblast cell conformational freedom of the collagen molecules.

No direct correlation between the hydrophilicity/surface roughness and fibroblast cells initial interaction is found because of simultaneous influence of other factors such as surface chemical composition and topography.

This multistep procedure to biofunctionalization of strong hydrophobic chemically inert polymer surfaces has a potential to be used whenever need arises to control cellular interaction with the siloxane rubber, for example at tissue engineering, cell culture, or biointegratable biomaterial development.

GKSS Institut für Chemie, Teltow, where AFM was performed is also gratefully acknowledged.

References

1. Baquey, Ch.; Palumbo, F.; Porte-Durrieu, M. C.; Legeay, G.; Tressoud, A.; D'Agostino, R. Nucl Instr Method Phys Res 1999, B151, 255.
2. Chan, C. M.; Ko, T.-M.; Hiraoka, H. Surf Sci Rep 1996, 24, 1.
3. Abbasi, F.; Mirzadeh, A.; Katbab, A.-A. Polym Int 2001, 50, 1279.
4. Chu, P. K.; Chen, J. Y.; Wang, L. P.; Huang, N. Mater Sci Eng 2002, R36, 143.
5. Lee, Sh.-D.; Hsue, G..-H.; Kao, Ch.-Y.; J Polym Sci Part A: Polym Chem 1996, 34, 141.
6. Satriano, C.; Konte, E.; Marletta, G. Langmuir 2001, 17, 2243.
7. Satriano, C.; Carpazza, S.; Guglielmino, S.; Marleta, G. Langmuir 2002, 18, 9469.
8. Vladkova, T.; Keranov, I.; Altankov G. In Proceedings of the fourth International Conference ICOSECS, Belgrade, Serbia, July 18–21, 2004; p 629.
9. Vladkova, T.; Keranov, I.; Dineff, P.; Altankov, G. In Proceedings of the XVIIIth Congress of Chemists and Technologists of Macedonia, Ohrid, Sept. 21–25, 2004; p 16.
10. Vladkova, T.; Katukojvala, S.; Greenberg, R.; Williams, L. J. Nucl Instr Method Phys Res 2005, B236, 552.
11. Keranov, I.; Vladkova, T.; Minchev, M.; Kostadinova, A.; Altankov, G.; Dineff, P. J Appl Polym Sci, to appear.
12. Shangguan, N.; Kerano, I.; Dineff, P.; Youroukov, S.; Avramova, I.; Krasteva, N.; Altankov, G. J Am Chem Soc 2003, 125, 7775.
13. Ho, C.-P.; Yasuda, H. J Appl Polym Sci 1990, 39, 154.
14. Scofield, J. H. J Electron Spectrosc 1976, 8, 129.
15. Bikerman, J. J. Ind Eng Chem 1941, 13, 443.
16. Fowkes, F. M. Ind Eng Chem 1964, 56, 40.
17. Chan, Ch.-M. Polymer Surface Modification and Characterization (SPE Book); Hanser, 1994.
18. Garbassi, F.; Morra, M.; Occhiello, E. Polymer Surfaces from Physics to Technology; Wiley: Chichester, 1994.
19. Ayad, S.; Boot-Handford, R. P.; Humphries, M. J.; Kadler, K. E.; Shuttleworth, C. A. The Extra Cellular Matrix: Facts Book, 2nd ed.; Academic Press: London, 1998.
20. Encyclopaedia of amino acids: beauty care and amino acids. Available at: www.ajinomoto.com/amino/eng/beauty_print.html.
21. Chen, H.; Brook, M. A.; Scheardown, H. Biomaterials 2004, 25, 2273.
22. Altankov, G. Interaction of Cells with Biomaterial Surfaces, DSc Thesis; Institute of Biophysics, BAS: Sofia, 2003.
23. Vladkova, T.; Krasteva, N.; Kostadinova, A.; Altankov, G. J Biomater Sci 1999, 10, 609.